Available online at www.sciencedirect.com

SCIENCE DIRECT®

ELSEVIER International Communications in Heat and Mass Transfer 32 (2005) 107–115

International Communications in HEAT and MASS TRANSFER

www.elsevier.com/locate/ichmt

Turbulent kinetic energy distribution across the interface between a porous medium and a clear region☆

Marcelo J.S. de Lemos*

Departamento de Energia-IEME, Instituto Tecnológico de Aeronáutica-ITA, 12228-900 São José dos Campos, SP, Brazil

Abstract

For hybrid media, involving both a porous substrate and an unobstructed flow region, difficulties arise due to the proper mathematical treatment given at the macroscopic interface. The literature proposes a jump condition in which shear stresses on both sides of the interface are not of the same value. This paper presents numerical solutions for such hybrid medium, considering here a channel partially filled with a porous layer through which an incompressible fluid flows in turbulent regime. Here, diffusion fluxes of both momentum and turbulent kinetic energy across the interface present a discontinuity in their values, which is based on a certain jump coefficient. Effects of such parameter on mean and turbulence fields around the interface region are numerically investigated. Results indicate that depending on the value of the stress jump parameter, a substantially different structure for the turbulent field is obtained.

Keywords: Interface; Jump conditions; Turbulence; Porous media; Environmental flows

1. Introduction

The study of important environmental and engineering flows can benefit from more realistic mathematical modeling. For example, grain storage and drying as well as flows over forests and vegetation can be characterized by some sort of porous structure through which a fluid permeates. Accordingly, when the domain of analysis presents a macroscopic interfacial area between a porous

☆ Communicated by J.P. Hartnett and W.J. Minkowycz.
* Tel.: +55 12 3947 5860; fax: +55 12 3947 5842.
E-mail address: delemos@mec.ita.br.

0735-1933/$ - see front matter © 2004 Elsevier Ltd. All rights reserved.
doi:10.1016/j.icheatmasstransfer.2004.06.011

medium and a clear flow region, the literature proposes the existence of a stress jump interface condition between the two media [1,2]. Analytical solutions involving such models have been published [3–5].

In addition, purely numerical solutions for two-dimensional hybrid medium (porous region-clear flow) in an isothermal channel have been considered in [6] based on the turbulence model proposed in [7,8]. That work has been developed under the double-decomposition concept [9–11]. Non-isothermal flows in channels past a porous obstacle [12] and through a porous insert have also been reported [13]. In all previous work of [6,12,13], the matching condition at the interface considered a continuous function for the stress field.

Recently, Refs. [14–17] presented numerical solutions for laminar and turbulent flow in a channel partially filled with a flat layer of porous material. Flows over wavy interfaces were also computed for both laminar [18] and turbulent flows [19]. There, the authors made use of the shear stress jump condition at the interface. Those works were based on a numerical methodology specifically proposed for hybrid media [6,12,13].

Another line of research on turbulent flow over permeable media is based on the assumption that within the porous layer the flow remains laminar [20–23], which, in turn, precludes application of such methodology to flows through highly permeable media (e.g. atmospheric boundary layer over forests or crop fields).

As seen, all of the above considered either a flat or a rough (wavy) interface limiting the porous substrate. The stress jump condition for the momentum equations was applied, but in all publications so far, no such flux discontinuity for the $\langle k \rangle^{v}$-equation has been considered. Motivated by that, Ref. [24] proposed a model that assumes diffusion fluxes of turbulent kinetic energy on both sides of the interface to be unequal, which differs from all studies presented up to now. The purpose of this paper is to further document and explore such proposal.

2. Macroscopic model

2.1. Geometry and governing equations

The flow under consideration is schematically shown in Fig. 1 where a channel is partially filled with a layer of a porous material. Constant property fluid flows longitudinally from left to right permeating through both the clear region and the porous structure. The channel section shown in the figure has length and height given by L and H, respectively. The channel is assumed to be long enough so that fully

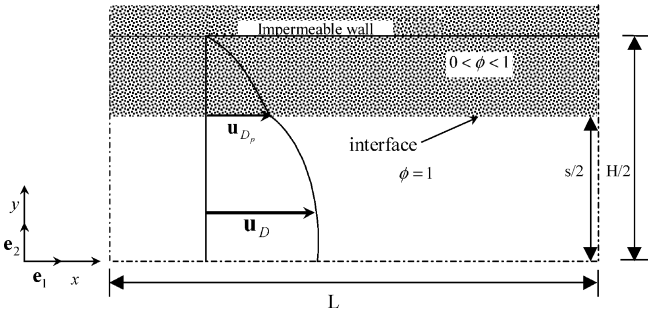

Fig. 1. Channel section with porous layer.

developed flow is established. Under this condition, variable profiles along y at x=0 are coincident to those at x=L.

A macroscopic form of the governing equations is obtained by taking the volumetric average of the entire equation set. In this development, the porous medium is considered to be rigid and saturated by the incompressible fluid. This equation set is already available in the open literature [17] and details do not need to be repeated here. Nevertheless, for the sake of completeness, the final form of the equations is here presented.

The macroscopic continuity equation is given by,

$$\nabla \cdot \overline{\mathbf{u}}_{\mathrm{D}} = 0 \tag{1}$$

where the Dupuit-Forchheimer relationship, $\overline{\mathbf{u}}_{\mathrm{D}}=\phi\langle\overline{\mathbf{u}}\rangle^{\mathrm{i}}$, has been used and $\langle\overline{\mathbf{u}}\rangle^{\mathrm{i}}$ identifies the intrinsic (liquid) average of the local velocity vector $\overline{\mathbf{u}}$ [25]. Eq. (1) represents the macroscopic continuity equation for an incompressible fluid in a rigid porous medium [26].

The macroscopic time-mean Navier-Stokes (NS) equation for an incompressible fluid with constant properties can be written as (see Ref. [7]) for details),

$$\rho\nabla\cdot\left(\frac{\overline{\mathbf{u}}_{\mathrm{D}}\overline{\mathbf{u}}_{\mathrm{D}}}{\phi}\right) = -\nabla\left(\phi\langle\overline{p}\rangle^{\mathrm{i}}\right) + \mu\nabla^2\overline{\mathbf{u}}_{\mathrm{D}} + \nabla\cdot\left(-\rho\phi\langle\overline{\mathbf{u}'\,\mathbf{u}'}\rangle^{\mathrm{i}}\right) - \left[\frac{\mu\phi}{K}\overline{\mathbf{u}}_{\mathrm{D}} + \frac{c_{\mathrm{F}}\phi\rho|\overline{\mathbf{u}}_{\mathrm{D}}|\overline{\mathbf{u}}_{\mathrm{D}}}{\sqrt{K}}\right] \tag{2}$$

where μ is the fluid dynamic viscosity, K is the permeability, c_{F} is the Forchheimer coefficient and $-\rho\phi\langle\overline{\mathbf{u}'\,\mathbf{u}'}\rangle^{\mathrm{i}}$ is the Macroscopic Reynolds Stress Tensor (MRST) modeled as:

$$-\rho\phi\langle\overline{\mathbf{u}'\,\mathbf{u}'}\rangle^{\mathrm{i}} = \mu_{t_\phi}2\langle\overline{\mathbf{D}}\rangle^{\mathrm{v}} - \frac{2}{3}\phi\rho\langle k\rangle^{\mathrm{i}}\mathbf{I} \tag{3}$$

Further,

$$\langle\overline{\mathbf{D}}\rangle^{\mathrm{v}} = \frac{1}{2}\left[\nabla\left(\phi\langle\overline{\mathbf{u}}\rangle^{\mathrm{i}}\right) + \left[\nabla\left(\phi\langle\overline{\mathbf{u}}\rangle^{\mathrm{i}}\right)\right]^{T}\right] \tag{4}$$

is the macroscopic deformation tensor, $\langle k\rangle^{\mathrm{i}}$ is the intrinsic average for k and μ_{t_ϕ} is the macroscopic turbulent viscosity, which is modeled here similarly to the case of clear fluid flow. A proposal for μ_{t_ϕ} was presented in [7] as,

$$\mu_{t_\phi} = \rho c_\mu\langle k\rangle^{\mathrm{i}^2}/\langle\varepsilon\rangle^{\mathrm{i}} \tag{5}$$

2.2. Macroscopic equations for turbulence

Transport equations for $\langle k\rangle^{\mathrm{i}} = \langle\overline{\mathbf{u}'\cdot\mathbf{u}'}\rangle^{\mathrm{i}}/2$ and $\langle\varepsilon\rangle^{\mathrm{i}} = \mu\langle\overline{\nabla\mathbf{u}' : (\nabla\mathbf{u}')^{T}}\rangle^{\mathrm{i}}/\rho$ in their so-called High Reynolds Number form are presented in [7] as:

$$\rho\nabla\cdot\left(\overline{\mathbf{u}}_{\mathrm{D}}\langle k\rangle^{i}\right) = \nabla\cdot\left[\left(\mu + \frac{\mu_{t_\phi}}{\sigma_k}\right)\nabla\left(\phi\langle k\rangle^{\mathrm{i}}\right)\right] + P^{\mathrm{i}} + G^{\mathrm{i}} - \rho\phi\langle\varepsilon\rangle^{\mathrm{i}} \tag{6}$$

$$\rho\nabla\cdot\left(\overline{\mathbf{u}}_{\mathrm{D}}\langle\varepsilon\rangle^{\mathrm{i}}\right) = \nabla\cdot\left[\left(\mu + \frac{\mu_{t_\phi}}{\sigma_\varepsilon}\right)\nabla\left(\phi\langle\varepsilon\rangle^{\mathrm{i}}\right)\right] + c_1P^{\mathrm{i}}\frac{\langle\varepsilon\rangle^{\mathrm{i}}}{\langle k\rangle^{\mathrm{i}}} + c_2\frac{\langle\varepsilon\rangle^{\mathrm{i}}}{\langle k\rangle^{\mathrm{i}}}\left(G^{\mathrm{i}} - \rho\phi\langle\varepsilon\rangle^{\mathrm{i}}\right) \tag{7}$$

where the c's are constants, $P^{\mathrm{i}} = -\rho\langle\overline{\mathbf{u}'\,\mathbf{u}'}\rangle^{\mathrm{i}} : \nabla\overline{\mathbf{u}}_{\mathrm{D}}$ is the production rate of $\langle k\rangle^{\mathrm{i}}$ due to gradients of $\overline{\mathbf{u}}_{\mathrm{D}}$ and $G^{\mathrm{i}} = c_k\rho\phi\langle k\rangle^{\mathrm{i}}|\overline{\mathbf{u}}_{\mathrm{D}}|/\sqrt{K}$ is the generation rate of the intrinsic average of k due to the action of the porous matrix.

2.3. Interface conditions

The equation proposed by [1,2] for describing the stress jump at the interface has been modified in [17] in order to consider turbulent flow, in the form,

$$\left(\mu_{\mathrm{eff}} + \mu_{t_\phi}\right)\frac{\partial\overline{u}_{\mathrm{D_p}}}{\partial y}\bigg|_{\text{Porous Medium}} - (\mu+\mu_t)\frac{\partial\overline{u}_{\mathrm{D_p}}}{\partial y}\bigg|_{\text{Clear Fluid}} = (\mu+\mu_t)\frac{\beta}{\sqrt{K}}\overline{u}_{\mathrm{D_p}}\bigg|_{\text{interface}} \tag{8}$$

where $\mathbf{u}_{\mathrm{D_p}}$ is the Darcy velocity component parallel to the interface, μ_{eff} is the effective viscosity for the porous region, and β an adjustable coefficient that accounts for the stress jump at the interface. Continuity of velocity, pressure, statistical variables and their fluxes across the interface are given by (see Ref. [17] for details),

$$\bar{\mathbf{u}}_{\mathrm{D}}\Big|_{\text{Porous Medium}} = \bar{\mathbf{u}}_{\mathrm{D}}\Big|_{\text{Clear Fluid}} \tag{9}$$

$$\langle\bar{p}\rangle^{\mathrm{i}}\Big|_{\text{Porous Medium}} = \langle\bar{p}\rangle^{\mathrm{i}}\Big|_{\text{Clear Fluid}} \tag{10}$$

$$\langle k\rangle^{\mathrm{v}}\Big|_{\text{Porous Medium}} = \langle k\rangle^{\mathrm{v}}\Big|_{\text{Clear Fluid}} \tag{11}$$

$$\left(\mu + \frac{\mu_{t_\phi}}{\sigma_k}\right)\frac{\partial\langle k\rangle^{\mathrm{v}}}{\partial y}\bigg|_{\text{Porous Medium}} = \left(\mu + \frac{\mu_t}{\sigma_k}\right)\frac{\partial\langle k\rangle^{\mathrm{v}}}{\partial y}\bigg|_{\text{Clear Fluid}} \tag{12}$$

$$\langle\varepsilon\rangle^{\mathrm{v}}\Big|_{\text{Porous Medium}} = \langle\varepsilon\rangle^{\mathrm{v}}\Big|_{\text{Clear Fluid}} \tag{13}$$

$$\left(\mu + \frac{\mu_{t_\phi}}{\sigma_\varepsilon}\right)\frac{\partial\langle\varepsilon\rangle^{\mathrm{v}}}{\partial y}\bigg|_{\text{Porous Medium}} = \left(\mu + \frac{\mu_t}{\sigma_\varepsilon}\right)\frac{\partial\langle\varepsilon\rangle^{\mathrm{v}}}{\partial y}\bigg|_{\text{Clear Fluid}} \tag{14}$$

Eqs. (9) and (10) were also proposed by [1] whereas relationships (11) (12) (13) (14) were used by [27].

3. A proposal for a diffusion flux jump for $\langle k\rangle^{\mathrm{v}}$ at the interface

In Ref. [17], no "jump" condition was considered when treating the diffusion flux of $\langle k\rangle^{\mathrm{v}}$ across the interface, as can be seen by Eq. (12). Here, in order to account for some extra effect in the transport

of $\langle k\rangle^{\mathrm{v}}$ between the two media, a discontinuity of the diffusion flux is considered. Such discontinuity might be due to interface roughness or be a way to comply with irregular interfaces. In addition, it can also be seen as an accommodation of the fact that close to the interface the permeability K attains higher values than those used within the porous substrate. For that, the following interface condition is here proposed,

$$\left(\mu_{eff}+\frac{\mu_{t_\phi}}{\sigma_k}\right)\frac{\partial\langle k\rangle^{\mathrm{v}}}{\partial y}\bigg|_{\text{Porous Medium}}-\left(\mu+\frac{\mu_t}{\sigma_k}\right)\frac{\partial\langle k\rangle^{\mathrm{v}}}{\partial y}\bigg|_{\text{Clear Fluid}}=(\mu+\mu_t)\frac{\beta}{\sqrt{K}}\langle k\rangle^{\mathrm{v}}\bigg|_{\text{Interface}} \tag{15}$$

instead of Eq. (12). Condition (15) is imposed along the interface shown in Fig. 1.

4. Numerical details

In Ref. [16], the discretization methodology used for including the jump condition in the numerical solutions was discussed in detail. For that, only brief comments about the numerical procedure are here made. Transport equations are discretized in a generalized coordinate system η–ξ using the control volume method [28]. Faces of the volume are formed by lines of constant coordinates η–ξ. The use of the spatially periodic boundary condition along the x coordinate was also discussed in [16,17]. This was done in order to simulate fully developed flow. The spatially periodic condition was implemented by running the 2D solution repetitively, until outlet profiles in $x=L$ matched those at the inlet ($x=0$). All computations were carried out until normalized residues of the algebraic equations were brought down to 10^{-6}. Details of the discretization of the terms on the left of Eq. (8) can be found in [8]. Furthermore, information on the discretization of the right of (8) appears in [16] where more details can be found. The height of the channel section was takes as $H=0.1$ m.

5. Results and discussion

The flow in Fig. 1 was computed with the set of Eqs. (1), (2), (6) and (7) including constitutive Eq. (3) and the Kolmogorov-Prandtl expression (5). The wall function approach was used for treating the flow close to the walls. Simulation of the fully developed condition required the use of the spatially periodic condition mentioned earlier. For all runs here studied, a total of 51 nodes in the axial direction were used.

Fig. 2a presents numerical solutions for β varying from -0.5 to 0.5 for a fixed a fixed porosity $\phi=0.6$, permeability $K=4\times10^{-4}$ m^2 and $Re_{\mathrm{H}}=1\times10^5$. When condition (12) is used instead if (15), profiles for β change substantially as the factor β is varied (dashed lines), from a smooth variation across the interface for a negative β, to an abrupt change in the velocity profiles when $\beta>0$. For positive β values, the Darcy velocity $\overline{\mathbf{u}}_{\mathrm{D}}$ is slightly higher inside the permeable structure than at the interface, indicating that flow resistance at this position would be higher than everywhere across the porous layer. This seemingly unphysical result is not obtained when condition (15) is applied for $\langle k\rangle^{\mathrm{v}}$ (thicker solid line in Fig. 2a). In this case, velocities close to the wall region are higher than for $\beta=0$ ($y>0.064$ m), but around the interface no such minimum in the value of $\overline{\mathbf{u}}_{\mathrm{D}}$ is observed. For $\beta<0$ (thin lines with symbols) no substantial difference in the calculated profiles, with and without a jump condition for $\langle k\rangle^{\mathrm{v}}$, is observed.

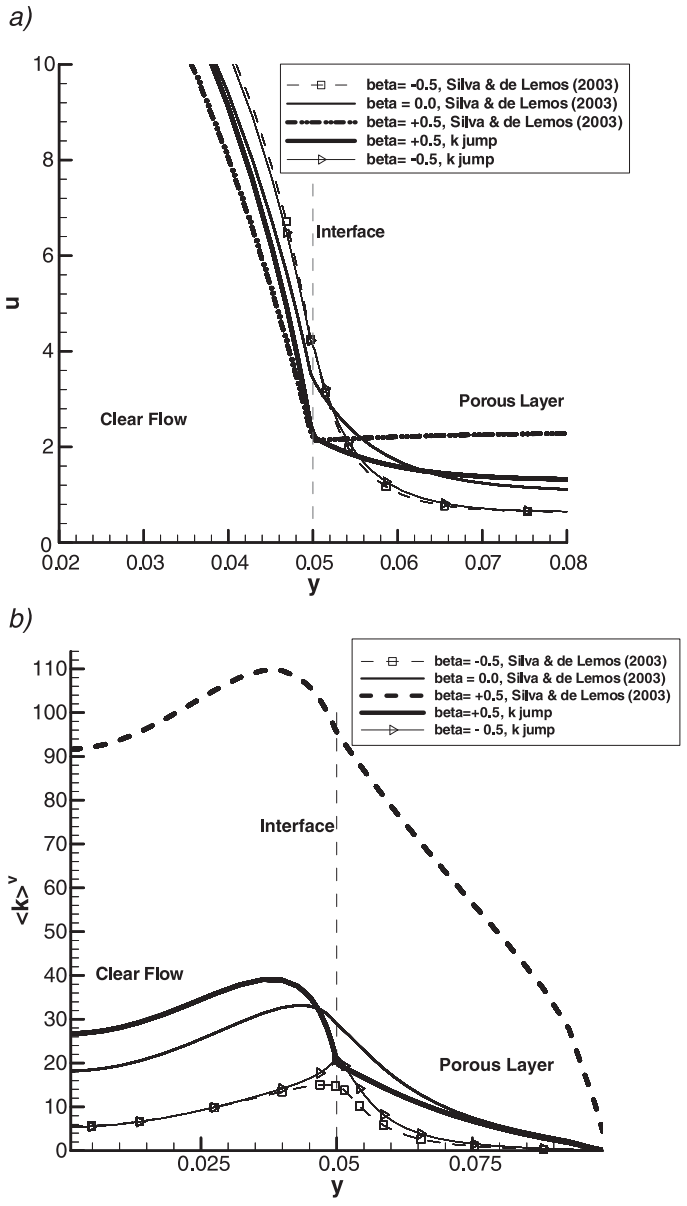

Fig. 2. Effect of parameter β on flow field: (a) mean velocity **u** [m/s]; (b) turbulent field, $\langle k \rangle^{v}$ [m^2/s^2].

Distributions for turbulent kinetic energy as a function of the interface boundary condition are shown in Fig. 2b. The clear separation for the two distributions for positive and negative values of β calculated by [17] (dashed lines) is not seen when interface condition (15) is applied (solid curves). The region of maximum turbulent kinetic energy is within the clear flow (y<0.05m) for β>0 (thicker solid line), whereas the use of a negative value for the jump parameter causes a peak for $\langle k \rangle^{v}$ to appear right at the interface (thin solid curve with symbols). Fig. 3 finally shows values for turbulent kinetic energy as a function of the jump parameter β. One can see a systematic behavior of larger values of $\langle k \rangle^{v}$ within the

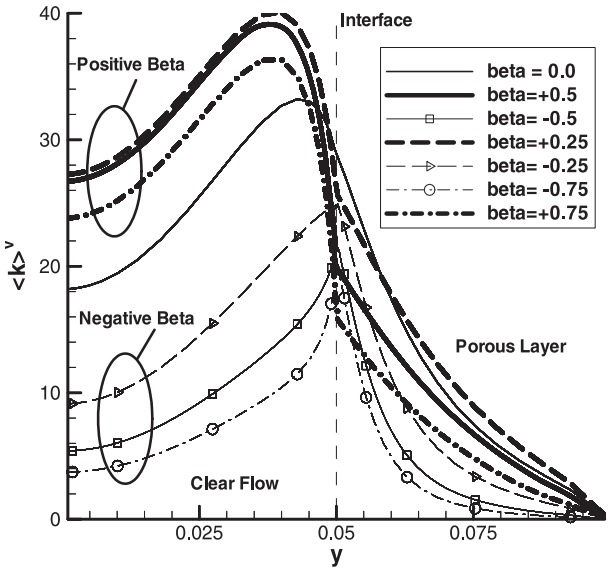

Fig. 3. Effect of β on turbulent field, $\langle k\rangle^{v}$ [m^2/s^2].

unobstructed layer for positive β values (thick lines) and its corresponding reduction when $\beta<0$ (thin curves). The peak in $\langle k\rangle^{v}$ profiles shifts from its position inside the clear flow for $\beta>0$ towards the interface for negative value of β. This is an indication that turbulence structure is substantially affected by the way the interface condition is modeled.

Ultimately, results in Figs. 2 and 3 indicate that for flows where interface condition (15) is applicable, the use of $\beta<0$ shows that a greater portion of the mean mechanical energy of the flow is converted into turbulence at the interface. If that is the case of environmental flows over dense and thick rain forests, for example, results herein might be useful to environmentalists and researchers analyzing important natural and engineering flows.

6. Conclusions

Numerical solutions for turbulent flow in a composite channel were obtained for different interface conditions for $\langle k\rangle^{v}$. Governing equations were discretized and solved for both domains making use of one unique numerical methodology. The use of a jump condition for the turbulent kinetic energy yielded numerical results substantially different from those of [17] where no such discontinuity in the diffusion fluxes of $\langle k\rangle^{v}$ across the interface was considered. Results herein may contribute to the analysis of important environmental and engineering flows where an interface surrounding a porous body is identified.

Nomenclature

A_t Transversal area of channel

c_F Forchheimer coefficient in Eq. (2)

c's Constants in Eqs. (5)–(7)
$\mathbf{D}$ Deformation rate tensor, $\mathbf{D}=[\nabla\mathbf{u}+(\nabla\mathbf{u})^T]/2$
G^{i} Production rate of $\langle k\rangle^{\mathrm{i}}$ due to the porous matrix, $G^{\mathrm{i}} = c_k\rho\phi\langle k\rangle^{\mathrm{i}}|\overline{\mathbf{u}}_{\mathrm{D}}|/\sqrt{K}$
H Distance between channel walls
k Turbulent kinetic energy per unit mass, $k = \overline{\mathbf{u}' \cdot \mathbf{u}'}/2$
$\langle k\rangle^{\mathrm{v}}$ Volume (fluid+solid) average of k
$\langle k\rangle^{\mathrm{i}}$ Intrinsic (fluid) average of k
K Permeability
L Channel length
p Thermodynamic pressure
$\langle p\rangle^{\mathrm{i}}$ Intrinsic (fluid) average of pressure p
P^{i} Production rate of k due to mean gradients of $\overline{\mathbf{u}}_D$, $P^{\mathrm{i}} = -\rho\langle\overline{u'\,u'}\rangle^{\mathrm{i}} : \nabla\overline{\mathbf{u}}_{\mathrm{D}}$
Re_{H} Channel height based Reynolds number, $Re_{\mathrm{H}}=(\rho|\overline{\mathbf{u}}_{\mathrm{D}}|H)/\mu$
$\overline{\mathbf{u}}$ Microscopic time-averaged velocity vector
$\langle\overline{\mathrm{u}}\rangle^{\mathrm{i}}$ Intrinsic (fluid) average of $\overline{\mathbf{u}}$
$\overline{\mathrm{u}}_{\mathrm{D}}$ Darcy velocity vector, $\overline{\mathbf{u}}_{\mathrm{D}}=\phi\langle\overline{\mathbf{u}}\rangle^{\mathrm{I}}$
$\overline{\mathbf{u}}_{\mathrm{D_p}}$ Darcy velocity vector parallel to the interface
$u_{\mathrm{D_n}}$, $u_{\mathrm{D_p}}$ Components of Darcy velocity at interface along η (normal) and ξ (parallel) directions, respectively.
x, y Cartesian coordinates

Greek
β Interface stress jump coefficient
μ Fluid dynamic viscosity
μ_{t} Turbulent viscosity
μ_{eff} Effective viscosity for a porous medium, $\mu_{\mathrm{eff}}=\mu/\phi$
μ_{t_ϕ} Macroscopic turbulent viscosity
ε Dissipation rate of k, $\varepsilon = \mu\overline{\nabla\mathbf{u}' : (\nabla\mathbf{u}')^T}/\rho$
$\langle\varepsilon\rangle^{\mathrm{I}}$ Intrinsic (fluid) average of ε
ρ Density
ϕ Porosity
η, ξ Generalized coordinates

Acknowledgments

The author is thankful to CNPq and FAPESP, Brazil, for their financial support during the course of this research.

References

[1] J.A. Ochoa-Tapia, S. Whitaker, Int. J. Heat Mass Transfer 38 (1995) 2635.
[2] J.A. Ochoa-Tapia, S. Whitaker, Int. J. Heat Mass Transfer 38 (1995) 2647.
[3] A.V. Kuznetsov, Int. J. Heat Fluid Flow 12 (1996) 269.

[4] A.V. Kuznetsov, Int. Commun. Heat Mass Transf. 24 (1997) 401.
[5] A.V. Kuznetsov, J. Porous Media 2 (3) (1999) 309.
[6] M.J.S. de Lemos, M.H.J. Pedras, Proc. IMECE2000-ASME-Intern. Mech. Eng. Congr., ASME-HTD-366-5, ASME, American Society of Mech. Engrs., New York, NY, USA, ISBN: 0-7918-1908-6, 2000 (Nov. 5–10) pp. 113–122 Orlando, FL.
[7] M.H.J. Pedras, M.J.S de Lemos, Int. J. Heat Mass Transfer 44 (6) (2001) 1081.
[8] M.H.J. Pedras, M.J.S de Lemos, Num. Heat Transfer-Part A 39 (1) (2001) 35.
[9] M.H.J. Pedras, M.J.S. de Lemos, On Volume and Time Averaging of Transport Equations for Turbulent Flow in Porous Media, ASME-FED-248, Paper FEDSM99-7273, ISBN 0-7918-1961-2 (1999).
[10] M.H.J. Pedras, M.J.S de Lemos, Int. Commun. Heat Mass Transf. 27 (2) (2000) 211.
[11] F.D. Rocamora Jr., M.J.S de Lemos, Int. Commun. Heat Mass Transf. 27 (6) (2000) 825.
[12] F.D. Rocamora Jr., M.J.S. de Lemos, Laminar Recirculating Flow And Heat Transfer In Hybrid Porous Medium-Clear Fluid Computational Domains, Proc. 34th ASME-National Heat Transfer Conf. (on CD-ROM), ASME-HTD-I463CD, Paper NHTC2000-12317, ISBN 0-7918-1997-3, Pittsburgh, Pennsylvania, Aug. 20-22 (2000).
[13] F.D. Rocamora Jr., M.J.S. de Lemos, Proc IMECE2000 - ASME-Intern. Mech. Eng. Congr., ASME-HTD-366-5, ASME, American Society of Mech. Engrs., New York, NY, USA, ISBN: 0-7918-1908-6, 2000 (Nov. 5–10) pp. 191–195 Orlando, FL.
[14] M.J.S. de Lemos, R.A. Silva, Numerical treatment of the stress jump interface condition for laminar flow in a channel partially filled with a porous material, Proc. Fluid Engineering Division Summer Meeting-ASME-FEDSM'02 (on CD-ROM), Montreal, Quebec, Canada, July 14–18, 2002.
[15] M.J.S. de Lemos, R.A. Silva, Simulation of a turbulent flow in a channel partially occupied by a porous layer considering the stress jump at the interface, Proc. Fluid Engineering Division Summer Meeting-ASME-FEDSM'02 (on CD-ROM), Montreal, Quebec, Canada, July 14182002.
[16] R.A. Silva, M.J.S. de Lemos, Num. Heat Transfer-Part A 43 (6) (2003) 603.
[17] R.A. Silva, M.J.S. de Lemos, Int. J. Heat Mass Transfer 46 (26) (2003) 5113.
[18] R.A. Silva, M.J.S. de Lemos, Proc. COBEM2003-17th. Int. Congr. of Mech. Engineering, Paper 1528 (on CD-ROM), São Paulo, Brazil, Nov. 10–14, 2003.
[19] M.J.S. de Lemos, R.A. Silva, Proc. ASME-FEDSM2003-Fluids Engineering Division Summer Meeting, Paper FEDSM2003-45457 (on CD-ROM), Honolulu, Hawaii, USA, July 6–11, 2003.
[20] A.V. Kuznetsov, L. Cheng, M. Xiong, Num. Heat Transfer-Part A 42 (2002) 365.
[21] A.V. Kuznetsov, L. Cheng, M. Xiong, Heat Mass Transf. 39 (2003) 613.
[22] A.V. Kuznetsov, M. Xiong, Int. J. Therm. Sci. 42 (2003) 913.
[23] A.V. Kuznetsov, S.M. Becker, Int. Commun. Heat Mass Transf. 31 (1) (2004) 11.
[24] M.J.S. de Lemos, Proc. ICTEA -Int. Conf. Thermal Eng. Theory and Applications, Paper ICTEA-TF2-01, Beirut, Lebanon, May 31–June 4, 2004.
[25] W.G. Gray, P.C.Y. Lee, Int. J. Multiph. Flow 3 (1977) 333.
[26] S. Whitaker, Indust. Eng. Chem. 61 (1969) 14.
[27] K. Lee, J.R. Howell, Proc. 1987 ASME-JSME Thermal Eng. Joint Conf., vol. 2, 1987, pp. 377–386.
[28] S.V. Patankar, Numerical Heat Transfer and Fluid Flow, Hemisphere, New York, 1980.